ISBN: 978-3-95450-214-1 ISSN: 2673-5490 doi:10.18429/JACoW-IPAC2021-TUPAB304

PRELIMINARY INVESTIGATION OF THE NOISES AND UPDATES ON PHYSICS STUDIES OF FOFB IN HEPS

X. Y. Huang†, Y. Y. Wei, Y. Jiao, Key Laboratory of Particle Acceleration Physics and Technology, Institute of High Energy Physics, Beijing, China

Abstract

High Energy Photon Source (HEPS) is a Fourth-generation storage ring light source in China and is under construction. Noises, such as the ambient mechanical vibration and the power supply ripples of magnets, may induce large orbit motions of electron bunches and hence dramatically degrade the emitted photon beam quality. The effect of noises becomes significant and needs to be considered very carefully, especially when the emittances of the electron beam approach the diffraction limit of x-ray. For the HEPS, the noises are modelled and the total beam orbit motion is evaluated considering the spectral characteristics of all the transformation processes from the errors to the orbit. In this paper, we present the preliminary calculation of the effects of noises in HEPS, and the control of the orbit motion with the FOFB system.

INTRODUCTION

The High Energy Photon Source (HEPS) is a 6-GeV storage ring light source being built in Beijing, China. To achieve the new requirements, the V3.0 lattice is adopted [1-3]. The optical functions and layout the lattice can be seen in Fig. 1. Although the modifications are not beneficial to emittance reduction and beam dynamics optimization, through optimization the horizontal natural emittance just has a little increase, from 34.2 pm·rad of the PDR design to 34.8 pm·rad of the new lattice, with large enough ring acceptance to meet the requirement of on-axis injection, with injected beam of smaller emittances thanks to re-optimization of the booster lattice.

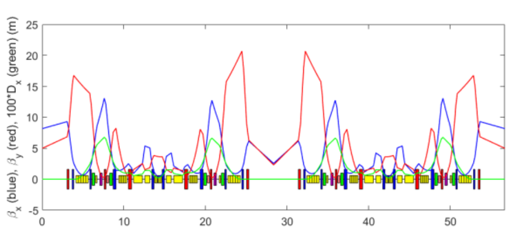

Figure 1: Layout of HEPS V3.0 lattice.

The orbit of HEPS storage ring will be affected by several kinds of noises, such as ambiance ground vibrations and power supply ripples. According to the beam stability requirements, the rms position/angular motion of the electron beam should be less than 10% of the beam size/divergence in both planes in the frequency range of DC ~ 500 Hz. For HEPS, some critical reference values of the orbit distortions for the final lattice are less than 1 μm and 0.3 μm in transverse and vertical plane, respectively.

In this paper, two major sources of the electron beam fluctuation are described: ground vibration and power supply noises. The ground vibration will drive the magnets vibration and cause the orbit motion. On the other hand, the power supply noises may induce the magnetic field fluctuation of the quadrupoles, slow correctors and fast correctors, which have impact to the orbit motion. There are other noise sources of the electron orbit motion, but most of them can be neglected.

The effect of a noise can be expressed in terms of power spectral density (PSD), the PSD of a time-dependent signal $x(t)$ is

$$PSD(f) = \lim_{T\to\infty}\left(\int_{-T/2}^{T/2} x(t)e^{-i\omega t}\,dt\right)^2, \qquad (1)$$

where $\omega = 2\pi f$. The signal's motion variance can be obtained by the integral of the PSD in Eq. (1) within specific frequency range, see Eq. (2), i.e. from negative infinite to infinite,

$$x^2 = \int_{-\infty}^{\infty} PSD(f)\,df. \qquad (2)$$

In our analysis, the PSD of the total motion can be added by the PSD of vibration noise induced motion and of power supply noise induced motion. In addition, the motion variance can be calculated with the PSD integral.

In order to attenuate the fast fluctuation of the beam orbit, a fast orbit feedback system (FOFB) with the bandwidth up to 500 Hz is considered. In the following, with some measurement data and reasonable assumptions, we will calculate the orbit fluctuation influenced by the vibration and the electrical noises w/o a 500 Hz bandwidth FOFB model applied.

ORBIT DUE TO GROUND VIBRATION

The ground vibration was measured near HEPS tunnel, the PSD of vibration displacement from 1 Hz to 100 Hz was shown in Fig. 2, the corresponding rms motion is about 20 nm in both planes. The relation between the ground motion and the corresponding orbit motion is characterized by orbit amplification factors, the normalized frequency-independent amplification factors are about 50 in both planes. However, for different ground vibration wavelength, the amplification factors are not the same. For example, if the wavelength covers the whole storage ring, all the magnets and the BPMs are moving together, this will reduce the impact on the orbit motion of the ground vibration.

In our calculation, the frequency-dependent amplification factor is obtained by the ratio of closed orbit to magnets displacement with different coherence length (correlated to different vibration frequency). The simulation is similar to the procedure described in Ref [4]:

† email address: huangxy@ihep.ac.cn

ISBN: 978-3-95450-214-1 ISSN: 2673-5490 doi:10.18429/JACoW-IPAC2021-TUPAB304

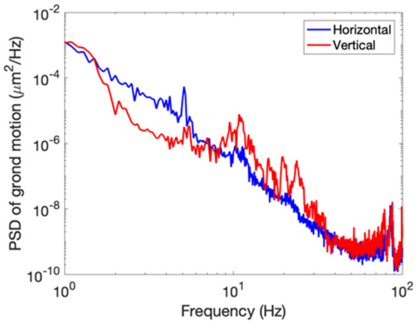

Figure 2: Measured PSD of the ground vibration in both planes.

Firstly, we generate the random Gaussian-distributed ground displacements in both planes. Secondly, we use the low-pass filter to smooth the random displacements, and the full width at the half maximum of the filter is defined as the coherence length. At last, the filtered displacements amplitude should be rescaled to the initial amplitude and subtract the average displacements. The filtered displacements for different coherence length are shown in Fig. 3.

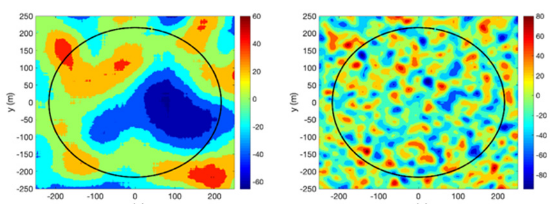

Figure 3: Displacements for different coherence length. The black dots indicate the magnets of HEPS storage ring.

With these ground vibration displacements, the magnet displacements can be calculated by sampling the ground displacement at the locations of the magnetic elements with interpolation. One should notice that the displacements of the magnets on the same girder need be linear fitted, and the horizontal displacements of a magnet need be transformed based on its' direction, see in Fig. 4.

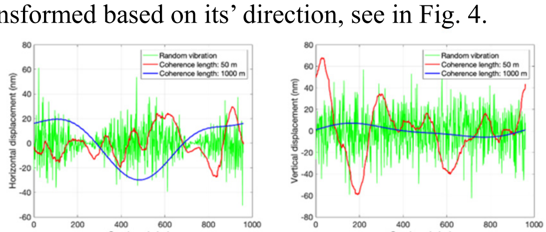

Figure 4: The quadrupole displacements with different coherence length in horizontal and vertical planes.

Then the amplification factor can be calculated by the ratio of the rms orbit motion at the source point to the ground displacements by averaging over 200 sets for each coherence length. The results are showing on Fig. 5. The left figure shows the amplification factor for each coherence length, and the right figure for the related frequency. Until now, we have not completed the measurement of the coherence of ground motion as a function of distance, so we use the approximation in Eq. (3) of the dependence of coherence length on frequency in Ref [4]:

$$L_x \approx 100/f^{1.1} \,\&\, L_y \approx 125/f^{1.4}. \quad (3)$$

In our simulations, the amplification factor saturation seen at large correlation lengths is explained by the orbit simulation accuracy when doing the interpolation. When calculating the expected orbit motion later, this saturating portion of the amplification factor dependence was replaced by a $1/L^2$ extrapolation.

With the amplification factors for each frequency, we can calculate the total orbit motion due to vibration noises. The total expected orbit motion due to ground vibration will be 0.02 µm in horizontal and 0.04 µm in vertical planes.

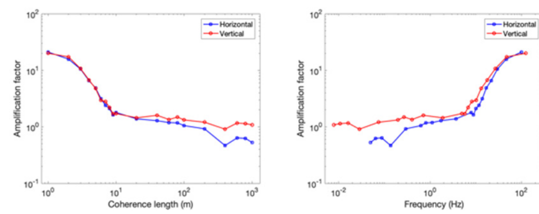

Figure 5: The amplification factor for each coherence length (left) and correlated frequency (right).

ORBIT DUE TO ELECTRICAL NOISE

In HEPS, orbit will be affected by the power supply noise in quadrupoles, slow correctors and fast correctors. The total effect of the magnets in one type can be calculated as

$$q_{rms}^2 = \sum \frac{\theta_{rms}^2}{4 \sin \pi v^2} \beta \beta_{ID} \cos(\phi - \pi v)^2, \quad (4)$$

in which q stands for the orbit in horizontal or vertical, and θ is the magnetic field error caused by power supply noise. For quadrupoles,

$$\theta_{rms} = \frac{\Delta I_{rms}}{I_{OP}} K_1 L u_{rms}, \quad (5)$$

where K_1 is the strength of the quadrupole, and I_{op} is the operation current. For correctors,

$$\theta_{rms} = \frac{\Delta I_{rms}}{I_{max}} \theta_{max}. \quad (6)$$

With these above equations, the amplification factors for different types of magnets can be calculated, see in Table 1, and the corresponding orbit motion of 1.38 µm in horizontal plane and 0.43 µm in vertical plane, respectively.

Table 1: The Calculated Amplification Factors for Different Types of Magnets

Magnet	Ax	Ay	Noise
Quadrupole	0.002	0.002	10 ppm
Slow Corrector	0.01	0.006	50 ppm
Fast Corrector	0.008	0.007	50 ppm

THE OVERALL ORBIT MOTION

The PSD of the total orbit motion can be summed by the PSD of the motion induced by the vibration noise and induced by the electrical noise. The overall rms orbit motion contributed by the two noise sources are 1.38 μm in horizontal and 0.44 μm in vertical planes, respectively, see in Fig. 6. One can see that the electrical noises dominant in the frequency range we care about.

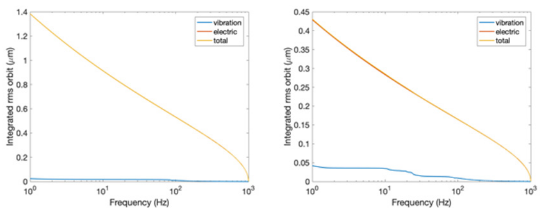

Figure 6: PSD of the total orbit motion in horizontal and vertical plane.

The ideal feedback loop can be modeled as

$$A_{fb} = \sqrt{2f^2/(f^2+f_0^2)}, \tag{7}$$

where f_0 is the efficient bandwidth of the feedback. If the efficient bandwidth is 500 Hz, the orbit motion can be attenuated to 0.41 μm in horizontal and 0.13 μm in vertical planes, which satisfies the stability requirement of HEPS, see in Fig. 7.

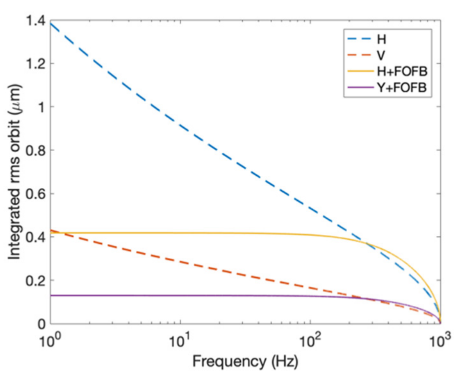

Figure 7: The integrated rms orbit motion w/o FOFB.

THE UPDATES OF FOFB

In this section, we present the latest structure design of the FOFB. As sketched in Fig. 8, the system will adopt hybrid communication with ring architecture. In our design, the FOFB system contains 48 local cell controllers, which are fairly well distributed around the storage ring. Each controller receives 48 local BPM FA data (22 kHz) and delivers them to other cell controllers by 10 Gbps fibre links. Then the cell controllers compute and distribute new power supply setpoints of eight local fast correctors in every 45 μs. Orbit feedback processing is based on a FPGA and multi-core DSPs integrated in each cell controller. SDI link and some data pre-processing are handled by the FPGA, while the DSPs performs the corrector setpoints computations by singular value decomposition (SVD) algorithm. The inverse response matrix is computed offline and will be uploaded to the cell controller as vector parameters in advance.

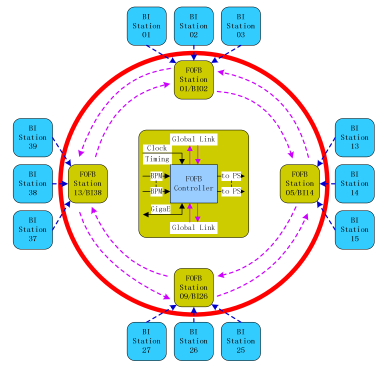

Figure 8: The structure of HEPS fast orbit feedback system.

CONCLUSION AND DISCUSSION

In this paper, according to our preliminary measurements and some reasonable assumptions, the orbit fluctuation due to vibration and power supply noises was estimated in HEPS storage ring. In our calculation, the magnet vibration is governed by the ground vibration and the amplification factor is decreased with the ground vibration wavelength enlarged, and the induced beam motion is negligible compared with the beam motion induced by power supply noises. The girder resonance was not included in our calculation. The measurements of ground vibration coherence and power supply noises were not completed, so some assumptions were made. The preliminary results show that the stability requirements can be achieved with FOFB. The detailed simulation of FOFB is still undergoing.

ACKNOWLEDGEMENT

We wish to thank Z. Duan, D. H. Ji for the discussions and huge help they provided. Also thanks to C. X. Yin and B. C. Jiang from SSRF for the advices and discussions.

REFERENCES

[1] Y. Jiao *et al.*, "Progress of lattice design and physics studies on the High Energy Photon Source", presented at IPAC'21, Campinas, SP, Brazil, paper MOPAB053, this conference.

[2] G. Xu, *et al.*, "Recent physical studies for the HEPS project", in *Proc. IPAC'16*, Busan, Korea, May 2016, paper WEPOW026, pp. 2886-2888.

[3] Y. Jiao, *et al.*, "Status of HEPS lattice design and physics studies", in *Proc. SAP'17*, Jishou, China, Aug. 2017, paper MOBH2, pp. 7-9.

[4] V. Sajaev, "Determination of the ground motion orbit amplification factors dependence on the frequency for the APS upgrade storage ring", in *Proc. IPAC'18*, Vancouver, BC, Canada, May 2018, paper TUPMF012, pp. 1272-1275.